Order–Disorder Transition of Ionic Clusters in Ionomers

Kenji Tadano,† Eisaku Hirasawa,‡ Hitoshi Yamamoto,§ and Shinichi Yano*,§

Gifu College of Medical Technology, Ichihiraga, Seki, Gifu 501-32, Japan, and Technical Center, Du Pont-Mitsui Polychemicals Co. Ltd., Chikusa Kaigan 6, Ichihara, Chiba 299-01, Japan, and Department of Chemistry, Faculty of Engineering, Gifu University, Yanagido, Gifu 501-11, Japan. *Received February 25, 1988; Revised Manuscript Received May 27, 1988*

ABSTRACT: Thermal expansion and differential scanning calorimetric studies have been made for the complex Zn(II) salts with 1,3-bis(aminomethyl)cyclohexane [1,3-$(H_2NCH_2)_2C_6H_{10}$] of ethylene–methacrylic acid copolymer to clarify the structure and transition of ionic clusters. It was found that the ionic clusters are ordered assemblies of ionic groups (ionic crystallites) and show an order–disorder transition of first order near 330 K below the melting point of crystallites of polyethylene regions. The transition of ionic clusters undergoes a thermal hysteresis which is explained by a relaxational process from an ordered state to a disordered state.

Introduction

Ionomers are polymeric materials consisting of hydrophobic organic backbone chains and a small amount of ionic groups. Many of the ionomers investigated so far are copolymers containing a small amount of pendant metal carboxylate or sulfonate groups. The hydrophilic ionic groups are separated from the hydrophobic polymer matrix to form small ionic domains (ionic clusters). The presence of ionic clusters has been evidenced by means of various techniques such as small-angle X-ray scattering (SAXS), mechanical and dielectric measurements, electron microscopy, and etc.[1-4] The formation of ionic clusters profoundly influences the physical properties of ionomers. The improved tensile strength, impact resistance, and optical properties have attracted many polymer physicists to fundamental and applied researches. Despite much research effort, the colloidal size of ionic clusters has prevented elucidation of the morphological nature of ionic clusters. Several structural models for the ionic clusters have been proposed, mainly on the basis of SAXS studies, but a final conclusion has not yet been drawn.

Recently, some evidence concerning the arrangement of ions inside the ionic clusters has been found by the use of new techniques: Extended X-ray absorption fine structure (EXAFS) results of Cooper et al.[5,6] indicated the existence of some ordered structure in the ionic clusters for the Zn(II) salts of sulfonated polystyrene. Yamauchi and Yano[7,8] observed the presence of Mn–Mn bond lengths of about 5.6 Å in the highly neutralized Mn(II) salts of ethylene–acrylic acid copolymer by electron spin resonance (ESR) measurements, which suggests the existence of some structural arrangement between the Mn(II) salts. New and more detailed morphological studies of ionic clusters are necessary to understand the structure and properties of ionomers.

To date, various types of ionomers have been developed[1-4] but many of them are ionomers neutralized by metal cations (see A in Table I). Organic amine derivatives can be counterions to form ionomers of various types, since they can form different quaternary amine salts with acid groups attached to the backbone chains, as shown in B of Table I. Only a few papers have been reported on these systems;[9-11] Rees[10] found that aliphatic diamines react with ethylene–methacrylic acid copolymer (EMAA) to form ionic cross-links in the polymer matrix and that the addition of diamines increases the tensile strength and yield modulus. Weiss and Agawarl[11] measured melt viscosities for various monoamine salts of polypropylene-*graft*-acrylic acid as $R'COO^-NH_pR_q^+$. They found that the melt viscosity is affected by the chemical structure of the monoamine. Very recently, we reported dielectric and SAXS work on the complex Zn(II) salts of EMAA with 1,3-bis(aminomethyl)cyclohexane [1,3-$(H_2NCH_2)_2C_6H_{10}$] (BAC)[12,13] (EMAA–xZn–yBAC: x is the degree of neutralization by Zn and y is the equivalent ratio of BAC to carboxylic acid, where BAC is divalent). This system is a new type of ionomer in which the ionic group is a complex Zn(II) salt with BAC as shown in C of Table I. The addition of BAC to the Zn(II) salt promotes the formation of ionic clusters by the increased ionic nature of the Zn-$(BAC)_{1-4}$–$(COO)_2$ bond, compared with the rather covalent nature of the Zn–$(COO)_2$ bond. Our preliminary thermal expansion and differential scanning calorimetric (DSC) work on this system indicated the existence of an order–disorder transition inside the ionic clusters around 330 K below the melting point of the polyethylene crystalline region (T_m = 363 K).[14] The complex Zn(II) salts with bulky BAC cause the large change in the thermal expansion and DSC data which allowed us to detect the existence of the transition.

Table I
Types of Ionic Groups in Ionomers[a]

type	A	B	C
chem formula	$-(COO^-)_nM^{n+}$	$-COO^-H_pR_qN^+$	$-(COO^-)_n$-$M(H_rR_sN)_w]^{n+}$

[a] M^{n+}, metal cation; R, aliphatic or aromatic group; p, q, r, s, and w are integers, where $p + q = 4$ and $r + s = 3$.

The purpose of the present work is to study the structure and transition of ionic clusters in the EMAA–xZn–yBAC system and to elucidate the mechanism of the transition.

Experimental Section

The samples used here are listed in Table II. The EMAA is ACR-1560 of Du Pont–Mitsui Polychemicals Co. Ltd, the methacrylic acid content of which is 5.4 mol %. The Zn(II) and BAC salts were prepared by a melt reaction of EMAA and zinc oxide/BAC in an extruder at 410–490 K. The complex Zn(II) salts with BAC were synthesized by the melt reaction of a mixture of the Zn(II) salts and BAC by the same procedure as described above. The pellet samples obtained were reformed into sheets by compression molding at about 430 K and cooled to room temperature at a rate of about 30 K/min by circulation of cold water in the mold jacket.

The formation of the Zn(II)/BAC salts as shown in A/B in Table I was confirmed by IR spectra: As EMAA was neutralized with Zn(II)/BAC cation, the stretching vibration at 1700 cm^{-1} of COOH group in EMAA was depressed and the absorption at 1583 cm^{-1}, which is attributable to the asymmetric stretching vibration of COO group in the zinc carboxylate,[15] appeared and

† Gifu College of Medical Technology.
‡ Du Pont–Mitsui Polychemicals Co. Ltd.
§ Gifu University.

0024-9297/89/2222-0226$01.50/0

Table II
List of Samples

sample	deg of neutraliztn by Zn, %	BAC:carboxylic acid, equiv	mp, K	deg of crystallinity,[a] %	MFR,[b] deg min^{-1}
EMAA	0	0	364	27	60
EMAA–0.97BAC	0	0.97	364	11	34
EMAA–0.20Zn	20	0	366	21	14
EMAA–0.20Zn–0.97BAC	20	0.97	364	11	22
EMAA–0.20Zn–1.21BAC	20	1.21	363	12	32
EMAA–0.40Zn	40	0	365	19	3.1
EMAA–0.40Zn–0.97BAC	40	0.97	363	11	12
EMAA–0.60Zn	60	0	363	17	0.7
EMAA–0.60Zn–0.97BAC	60	0.97	362	14	4.7
EMAA–0.60Zn–1.21BAC	60	1.21	363	11	7.3

[a] The data were estimated from the heat of fusion by assuming that the heat of fusion of polyethylene crystallites is 290.4 J/g. [b] Melt flow rates under 2160 g load at 463 K.

increased. With the addition of BAC to the Zn(II) salts, the absorption peak at 1583 cm^{-1} for the Zn(II) salts was replaced by the absorption at 1564 cm^{-1}, which indicates the formation of the complex Zn(II) salts with BAC (see C in Table I). The syntheses of the complex Zn(II) salts with various organic amines were attempted by the same procedure as described above. When the organic amine formed the complex salts, it was stable in the polymer matrix and did not decompose below 373 K. When it did decompose the color of the film changed to brown and there was a strong smell. The present samples were stable above 373 K, which also suggests the formation of the complex salts.

DSC measurements were carried out with a Du Pont DSC-990 calorimeter at a heating/cooling rate of 10 K/min. Thermal expansions were measured at a heating/cooling rate between 0.3 and 0.6 K/min by the use of a glass dilatometer, in which the samples were carefully immersed in liquid Hg in vacuo to avoid a formation of voids on the surface of the sample. The change in volume of the sample with temperature was calculated from the readings of the height of Hg in the 0.6-mm-i.d. capillary of the dilatometer. The specific volume, V, at 298 K was obtained by a buoyancy method with benzene. Dielectric measurements were carried out with a multifrequency LCR meter (Hewlett-Packard, Type 4274A) equipped with a personal computer in a temperature range 85–390 K at several frequencies between 100 Hz and 100 kHz. Dynamic mechanical properties were measured by a Rheovibron (DV-II-C, Toyo Baldwin Co. Ltd.) at a heating rate of about 2 K/min in the temperature range from 90 to 350 K and at several frequencies between 3.5 and 110 Hz. Wide-angle X-ray scatterings (WAXS) were measured with Geiger–Müller counter using monochromatic Cu Kα radiation (Rigakudenki, Type Geiger Flex 2024).

Results and Discussion

Typical DSC curves are shown for EMAA–0.60Zn–0.97BAC in Figure 1. In the first heating, two endothermic peaks are observed near 331 and 362 K. The higher temperature peak clearly corresponds to the melting of polyethylene crystalline region in the polymer matrix. In the first cooling, one exothermic peak is observed near 317 K, corresponding to the crystallization of polyethylene chains. Apparently the lower temperature peak undergoes a thermal hysteresis; in the first heating, the peak appears near 331 K, but the peak is depressed in both the first cooling and second heating processes. Here the second heating is run soon after the first cooling. As the sample is stored at room temperature after the first cooling, the peak begins to appear upon heating, gradually shifts to higher temperatures, and becomes larger. The peak partially reverts to that of the original sample during the storage duration of about 38 days. Figure 2 shows DSC curves in the first heating for several samples. Two endothermic peaks are observed in all the samples. The lower temperature peaks shifts to slightly higher temperatures and becomes larger when BAC is added to the Zn(II) salts.

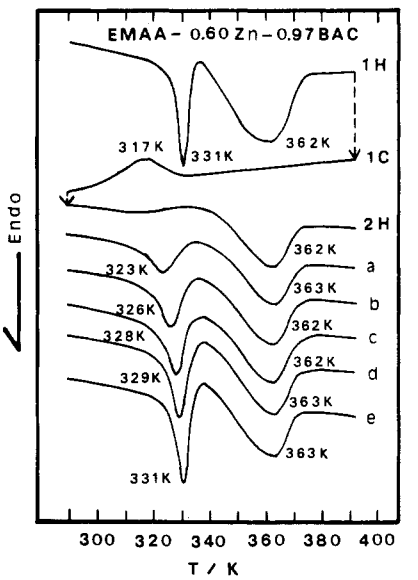

Figure 1. DSC curves for EMAA–0.60Zn–0.97BAC: 1H, first heating; 1C, first cooling; 2H, second heating; second heating processes after storing for (a) 5 h, (b) 1 day, (c) 3 days, (d) 9 days, and (e) 38 days at room temperature.

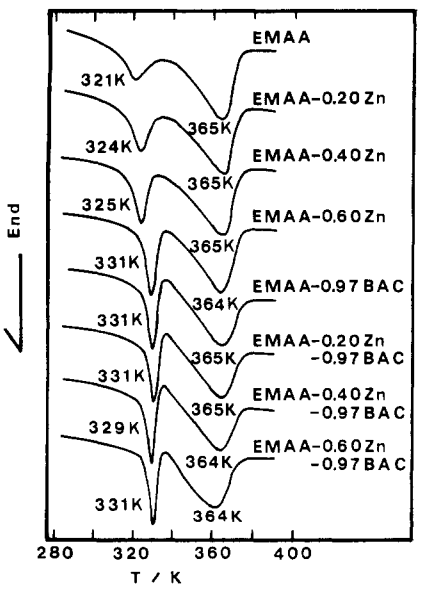

Figure 2. DSC curves in the first heating for various samples.

Plots of specific volume, V, versus temperature for several samples are shown in the temperature range from room temperature to 353 K below T_m in Figure 3 and to 393 K above T_m in Figure 4. In the sixth heating of Figure 4, one large increase of V takes place near 365 K by the

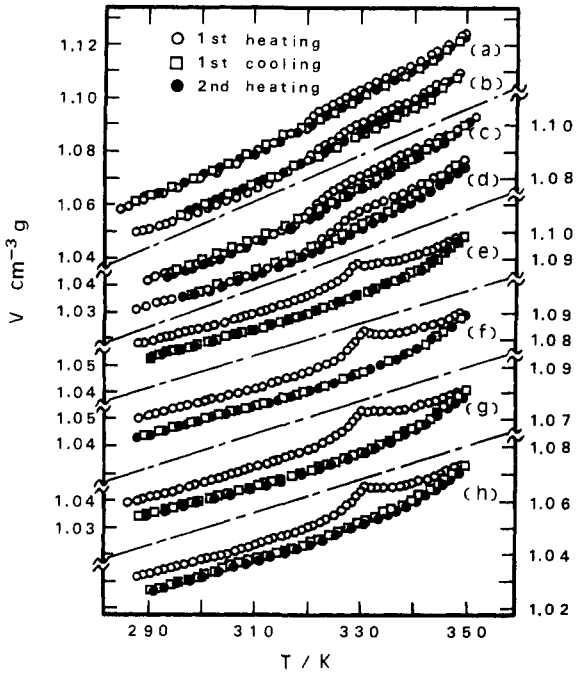

Figure 3. Plots of specific volume, V, versus temperature for several samples in the temperature range from room temperature to 353 K: (a) EMAA; (b) EMAA–0.20Zn; (c) EMAA–0.40Zn; (d) EMAA–0.60Zn; (e) EMAA–0.97BAC; (f) EMAA–0.20Zn–0.97BAC; (g) EMAA–0.40Zn–0.97BAC; (h) EMAA–0.60Zn–0.97BAC.

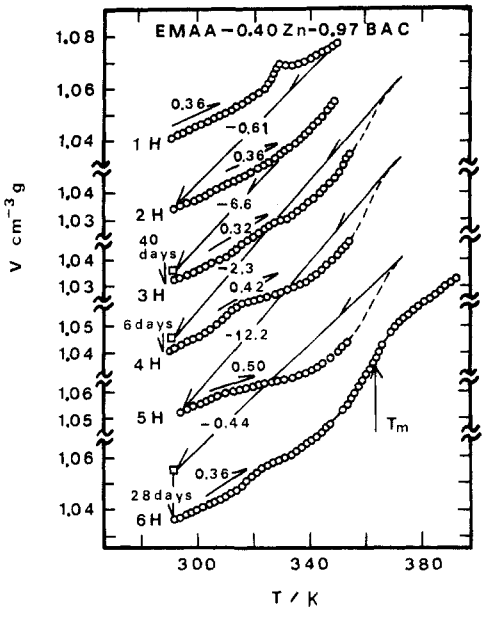

Figure 4. Plots of specific volume, V, versus temperature for EMAA–0.40Zn–0.97BAC in the temperature range from room temperature to 393 K: (O) data on heating, nth H, nth heating process by the heating rate (K/min) written near the plots: (—) mean quenching to room temperature by the cooling rates (K/min) written on the solid lines. n days: the storage days at the temperatures denoted by □.

melting of crystallites of polyethylene chains. In the first heating, one peak is observed near 331 K below T_m, corresponding to the lower temperature peak of the DSC curve. The peak undergoes the characteristic thermal hysteresis, similar to those in the DSC curve. In Figure 3, the thermal hysteresis is as follows: (1) In EMAA and the Zn(II) salts, the lower temperature peak appears as a small change in the first heating but is depressed in the first cooling and second heating. The value of V at room temperature scarcely changes by the thermal process. (2) In both the BAC salts and the complex Zn(II) salts with

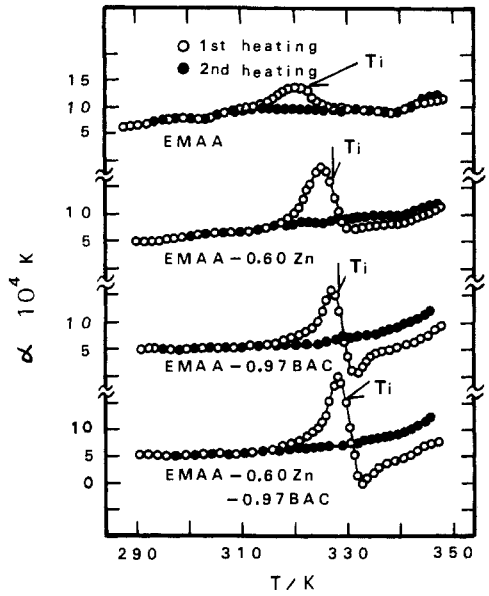

Figure 5. Plots of thermal expansion coefficient, α, versus temperatures for several samples. T_i: the transition temperature of ionic cluster obtained from Figure 3.

BAC, the thermal hysteresis is fundamentally the same as that of the Zn(II) salts. However, the lower temperature peaks in the first heating are larger in height, compared with those of the Zn(II) salts, and when the first cooling is performed, the value of V at room temperature is smaller than that of the original sample. The V–temperature curve for the second heating is almost the same as that for the cooling process. However, as the sample was stored at room temperature, in the second heating process, the lower temperature peak began to appear, shifted to higher temperatures, and gradually became larger.[14] In Figure 4, the lower temperature peak is also depressed in the second heating and begins to appear when the sample is stored at room temperature. The peak shifts to higher temperatures and is larger with increasing storage duration at room temperature. For the samples cooled from a temperature above T_m, the value of V at room temperature gradually decreases as the sample is stored at room temperature (for example, see 4H or 6H in Figure 4). This decrease in V may be caused by a crystallization of polyethylene chains, since the crystallization by cooling from the molten state is supercooled to around 317 K as shown in Figure 1. The thermal expansion coefficient (α) was calculated from the V–temperature plots of Figure 3 as follows: The value of α at one temperature was estimated by the use of the least-square polynomial method for seven data points involving measurements at three subsequent temperatures above and below the temperature. Plots of α versus temperature are shown in Figure 5. The value of α exhibits a peak near 330 K, corresponding to the lower temperature peak, which indicates a transition of the first order. Here, the transition temperature (T_i) was determined as the temperature exhibiting a maximum of the peak in the V–temperature plots. The values of T_i and α are listed in Table III. Both DSC and thermal expansion data apparently indicate the presence of a first-order transition near 330 K, because the transition is seen as an endothermic peak in the DSC curve and the discontinuous peak of the V–temperature plots. Furthermore, we concluded that this may be explained by an order–disorder transition of first order inside of the ionic clusters, from the following facts:

(1) The annealed EMAA–0.60Zn, EMAA–0.97BAC, and EMAA–0.60Zn–1.21BAC samples were prepared by cooling

Table III
Physical Data for the Order-Disorder Transition of Ionic Clusters

sample	T_m,[a] K	T_i,[b] K	α(298 K),[b] 10^{-4}/K	V(298 K),[c] cm^3/g
EMAA	365	321	7.78	1.0680
EMAA–0.20Zn	365	325	6.83	1.0558
EMAA–0.40Zn	365	323	6.26	1.0469
EMAA–0.60Zn	364	327	5.75	1.0368
EMAA–0.97BAC	365	328	4.70	1.0632
EMAA–0.20Zn–0.97BAC	365	327	4.69	1.0555
EMAA–0.40Zn–0.97BAC	364	330	4.93	1.0454
EMAA–0.60Zn–0.97BAC	362	330	5.06	1.0370

[a] The data were estimated from the DSC curves. [b] The data were estimated from the V–temperature plots for the first heating. [c] The data are for the original samples.

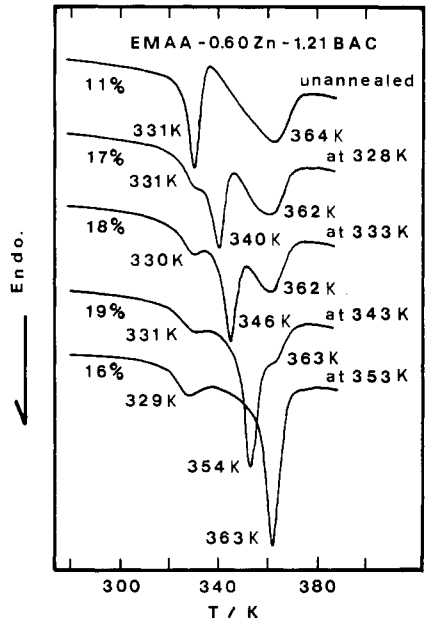

Figure 6. DSC curves in the heating process of EMAA–0.60Zn–1.21BAC annealed at several temperatures for 12 h. x%: degree of crystallinity of polyethylene region.

to room temperature at a cooling rate of 5 K/h, after they were annealed for 12 h at several temperatures between 328 and 353 K. DSC curves of the annealed EMAA–0.60Zn–1.21BAC samples are represented in Figure 6. Similar DSC curves were obtained for EMAA–0.60Zn and EMAA–0.97BAC In the unannealed sample, the two peaks, the lower temperature peak and the higher temperature peak, are observed at 331 and 364 K, respectively. After the sample is annealed, another new peak clearly appears. With increasing annealing temperature, the new peak shifts to higher temperatures and joins with the higher temperature peak at 353 K. The new peak may originate in the melting of so-called quasi-crystallites in polyethylene regions which are formed by annealing, since it appears at a temperature about 15 K higher than the annealing temperature. Furthermore, it is noted that T_i for the lower temperature peak does not change on annealing. This result indicates that the lower temperature peak does not come from the melting of the polyethylene crystalline region; if the lower temperature peak is related to the melting of the quasi-crystallites, it never exists at temperatures lower than the annealing temperature, but actually the lower temperature peak appears at 329 K, even when the annealing temperature is 353 K. Consequently, it seems to be valid that the lower temperature peak is not caused by the melting of crystallites of the polyethylene region.

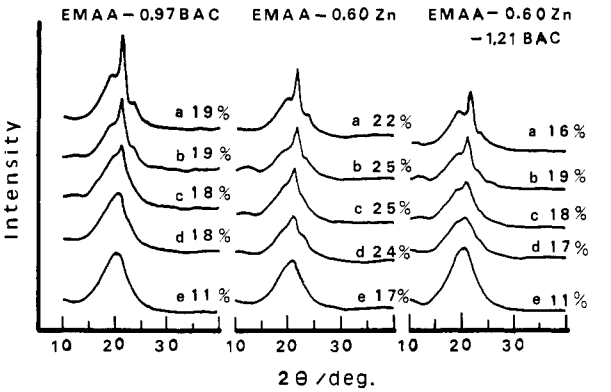

Figure 7. Intensity of wide-angle X-ray scattering versus scattering angle (2θ) for three samples annealed at several temperatures. Annealing time, 12 h; annealing temperature (a) 353 K, (b) 343 K, (c) 333 K, (d) 328 K, (e) unannealed. x%: degree of crystallinity of polyethylene region.

(2) As shown in Figure 3, both the thermal history and the type of salt exert a profound influence on the lower temperature peak. In EMAA–Zn–BAC and EMAA–BAC systems, the value of V at room temperature is lowered by experiencing the first heating process but remains constant in the EMAA–Zn systems. The lower temperature peak is depressed on both the first cooling and the second heating processes, as described already. In the first heating, the magnitude of the peak is bigger in EMAA–Zn–BAC and EMAA–BAC systems than in EMAA and EMAA–Zn systems. Change of degree of crystallinity in polyethylene regions by annealing is shown for EMAA–0.60Zn, EMAA–0.97BAC, and EMAA–0.60Zn–1.21BAC in Figure 7. The degree of crystallinity was roughly estimated from the sum of the heat of fusion for the quasi-crystallites and that for the higher temperature peak by assuming that the heat of fusion of polyethylene is 290.4 J/g. The degrees of crystallinity for the three samples increase by about 6% by annealing and the increase changes with neither annealing temperature nor type of salt. Nevertheless, the first heating process causes the decrease of V at room temperature for EMAA–BAC and EMAA–Zn–BAC systems but does not for EMAA–Zn, as mentioned above. The above results cannot be explained by the crystallization of polyethylene regions, since the increase in the crystallinity by annealing is almost the same in the three samples.

(3) In the V–temperature plots of Figures 3 and 4, the lower temperature peak is depressed by experiencing the first heating and begins to appear after storing the sample at room temperature. Usually the crystallization of polyethylene regions seems not to proceed easily at room temperature for samples cooled from a temperature below T_m. Moreover, melting of crystallites in polyethylene regions should be observed not as a peak but a discontinuous jump of V in V–temperature plots. Therefore the lower temperature peak may not come from the crystallization of polyethylene regions.

(4) Figure 7 shows plots of X-ray scattering intensity against scattering angle (2θ) for the samples annealed at several temperatures. The data exhibit a shallow peak for the unannealed sample and a new peak appears near 21° on annealing. The peak near 21° is clearly attributed to the [110] reflections from the crystallites of polyethylene regions (rhombic, D_{2h}^{16}).[16] The intensity of [110] reflection increases with increasing annealing temperature. However, the degree of crystallinity is not so much increased from DSC data as noted in Figure 7. In the unannealed sample, the polyethylene crystallites might be too small and too defective to detect the [100] reflections in the WAXS

curves. The imperfect and small crystallites may grow by annealing, and this may result in the appearance of the [100] reflection on WAXS curves. In the DSC curves of Figure 6, the higher temperature peak is very broad and the new peak produced by annealing is sharp. Consequently the annealing treatments seem not to increase the degree of crystallinity in polyethylene region strongly enough to affect the value of V noticeably.

(5) BAC-methacrylate crystals [$(CH_2{=}CMe{-}COO)_2BAC$] were prepared by mixing equimolar methacrylic acid and BAC in *n*-hexane at room temperature, and DSC measurements were performed on the crystals. In the first heating, one endothermic peak was observed near 410 K, corresponding to the melting point, but no peak was seen in the first cooling and second heating. When the crystals were stored for 7 days at room temperature after the first cooling, one endothermic peak appeared near 333 K and very gradually shifted to higher temperatures as the crystals are stored longer. The above melting behavior is very similar to that of the lower temperature peak in the present ionomers.

(6) We are progressing on EXAFS studies of the present ionomers.[17] At room temperature, the first coordination shell peak was observed at a radius of about 1.6 Å for EMAA-0.60Zn in the radial structural function—distance from Zn atom curves, which can be attributed to oxygen at a distance of 1.91 Å with four-folded coordination.[5] In EMAA-Zn-BAC systems, the Zn-O distance was slightly larger compared with that in EMAA-0.60Zn, and the first coordination shell peak was broader. At 378 K above T_i, the Zn-O distance was slightly shorter than that at room temperature in all the samples, unexpectedly. In EMAA-0.60Zn, furthermore, the shape of the first coordination shell peak at 378 K was almost the same as that at room temperature for EMAA-0.60Zn but was noticeably broader in EMAA-Zn-BAC systems, which indicates some disturbance in the local zinc cation environment. The disturbance and shortening of Zn-O distances seems to provide evidence for the order-disorder transition of ionic custers proposed in this work.

(7) The dielectric relaxation and mechanical results also support the presence of the order-disorder transition as described in detail later.

The existence of transitions of ionic clusters has been predicted by several researchers from the very small changes in DSC[18] and thermal expansion data,[19] but the evidence seems not to be convincing. Eisenberg and Trepman[19] found an unusual thermal hysteresis of the thermal expansion coefficient in styrene-sodium methacrylate copolymers; the value of the expansion coefficient above T_g is smaller in the first heating than in the first cooling and second heating processes. They assumed that this thermal hysteresis is caused by destruction of ionic clusters and a relaxational regeneration of the ionic clusters. Weiss[18] also assumed a transition of ionic clusters to explain the thermal hysteresis of the endothermic peak below T_m in the DSC curve of the Zn(II) salts of sulfonated polystyrene. Tsujita et al.[20,21] explained the thermal hysteresis in the DSC curve for ethylene-zinc/sodium methacrylate copolymer by a crystallization of polyethylene chains around the ionic clusters. Even if the decrease of V at T_i comes in part from crystallization of polyethylene regions, we think that this contribution to the V decrease is small. Since the size of ionic clusters is colloidal, it seems to be too difficult to directly demonstrate the presence of the order-disorder transition inside the ionic clusters. From our present results, however, we believe firmly in the existence of the transition.

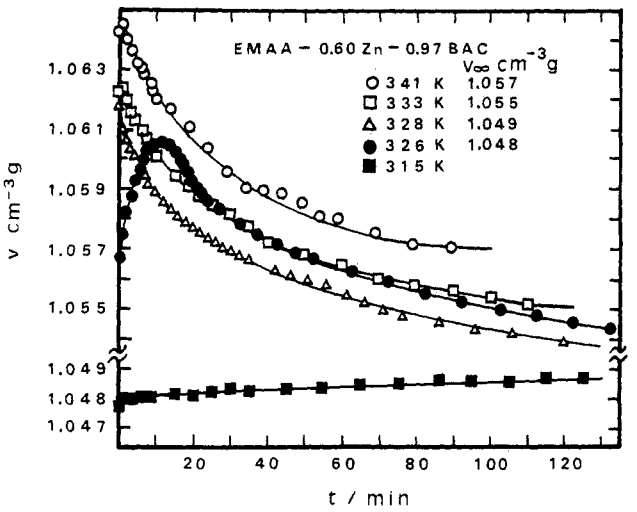

Figure 8. Plots of specific volume, V, versus annealing time, t, at several annealing temperatures for EMAA-0.60Zn-0.97BAC.

Generally, a first-order transition is seen as a discontinuous jump of V in V-temperature plots. In the present system, as temperature is increased, the value of V rapidly increases just below T_i by a pretransitional effect and gradually decreases above T_i as the temperature is increased. Therefore the transition is visualized as a peak in V. Unexpectedly, this peak suggests that the values of V in the disordered state above T_i are smaller than that in the ordered state. This unusual result can be understood by the following interpretation: Since BAC is bulky, the complex Zn(II) salts with BAC may form a voluminous structure inside the ionic clusters. The voluminous structure may cause the decrease of V due to the destruction of the order at T_i. Figure 8 shows change of V by the annealing time, t, at several temperatures. With increasing t, the value of V exponentially decreases above T_i but remains constant at 315 K below T_i. Therefore, the decrease of V may occur due to the destruction of order of ionic clusters, and the destruction is governed by a relaxational process as represented by the following equations.

$$\Delta V(t) = \Delta V_0 \exp(-t/\tau)$$

or

$$(V - V_\infty)/(V_0 - V_\infty) = \exp(-t/\tau)$$

Here, V_0, V_∞, and V are the values of V at annealing time of 0, ∞, and t, respectively. $\Delta V(t) = V - V_\infty$, $\Delta V_0 = V_0 - V_\infty$, and τ is relaxation time. On the other hand, the relaxational equation is also represented for the value of the transition enthalpy, ΔH, obtained by the DSC data as

$$\Delta(\Delta H)(t) = \Delta(\Delta H)(\infty)[1 - \exp(-t/\tau)]$$

or

$$(\Delta H - \Delta H_0)/(\Delta H_\infty - \Delta H_0) = 1 - \exp(-t/\tau)$$

Here, ΔH_0, ΔH_∞, and ΔH are the transition enthalpy at annealing times of 0, ∞, and t, respectively. $\Delta(\Delta H)(t)$ is the increase of ΔH at t. Plots of ln $[(V - V_\infty)/(V_0 - V_\infty)]$ versus t are shown in Figure 9. The plots consist of two straight lines and this result indicates that the relaxational change from the ordered state to the disordered state proceeds by two processes: a fast process (F process) and slower process (S process). Plots of ln $[1 - (\Delta H - \Delta H_0)/(\Delta H_\infty - \Delta H_0)]$ versus t are shown in Figure 10. These plots obey the two-relaxation process. Values of τ were 18 min at 341 K and 33 h at 301 K for the F process and 28 min at 341 K and 32 days at 301 K for the S process, respec-

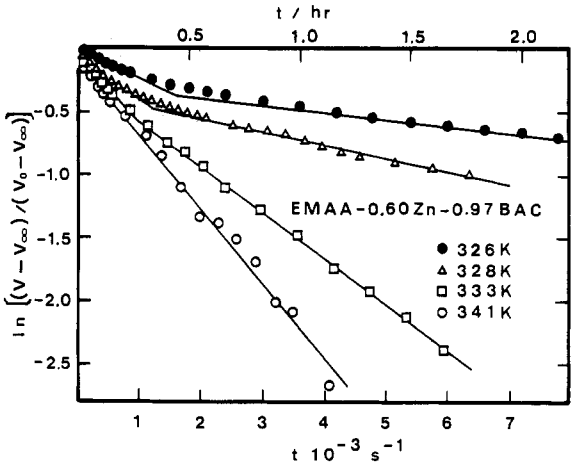

Figure 9. Plots of ln $[(V - V_\infty)/(V_0 - V_\infty)]$ versus annealing time, t, at several temperatures.

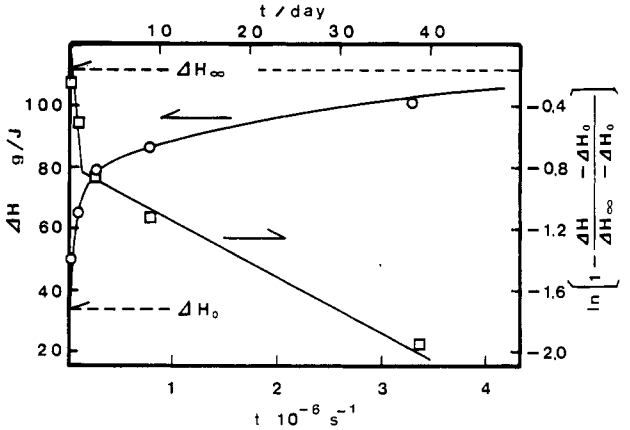

Figure 10. Plots of ΔH and ln $[1 - (\Delta H - \Delta H_0)/(\Delta H_\infty - \Delta H_0)]$ versus annealing time, t, at 301 K.

tively. Plots of ln $1/\tau$ against reciprocal temperature are shown in Figure 11 and satisfy a rate process

$$\ln 1/\tau = A - \Delta E/RT$$

Here, ΔE, R, and A are the activation energy, the gas constant, and the frequency factor, respectively. The values of ΔE were 110 and 170 kJ/mol for the F and S processes, respectively. The presence of the two relaxational processes leads to the following interpretation for the transition: In the ordered state, the crystallites in the ionic clusters may be in an equillibrium state associated with the polymer chains in the polymer matrix. When the crystallites are melted at T_i, the faster change to a disordered state of the ionic clusters (the F process) occurs first and the clusters are not connected with the polymer chains in the polymer matrix, and the second, slower change (the S process) may follow to reach an equilibrium state for the whole system which involves both the ionic clusters and the polymer matrix.

Figure 12 illustrates our model originating in the order–disorder transition of ionic clusters. The original sample consists of three phases: ionic clusters, a polyethylene crystalline region, and an amorphous region. When the temperature is increased from room temperature, the crystallike order inside the ionic clusters is destroyed at T_i, giving a disordered state, and on further increasing the temperature, the polyethylene crystallites melt at T_m but the disordered ionic clusters still exist. In the cooling process from the temperature above T_m, the crystallization of polyethylene regions take place at T_c, but the ordering in the ionic clusters does not appear down to

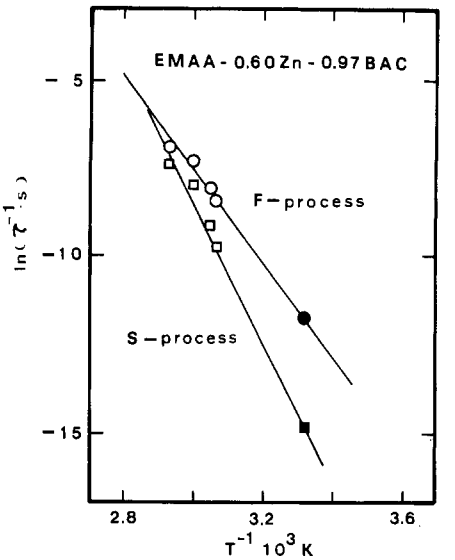

Figure 11. Plots of ln $1/\tau$ versus $1/T$ for EMAA–0.60Zn–0.97BAC.

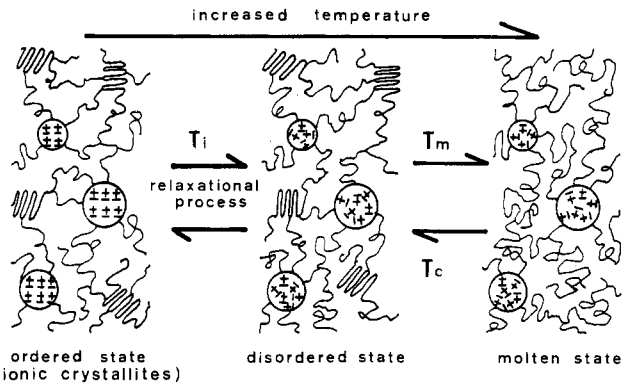

Figure 12. Model for order–disorder transition of ionic clusters.

room temperature. However, upon storing the sample below T_i, the disordered ionic clusters very slowly change to the ordered ones; this slow change results from the relaxational process with long relaxation time.

The existence of ionic clusters in ionomers has been evidenced experimentally and theoretically.[1-3] However, past structural analysis does not appear to have reached a convincing conclusion concerning the structure of ionic clusters becuse of their colloidal size and low concentration. Morphological studies of ionic clusters have been mainly done by SAXS measurements. The two models, two-phase model[22] and core–shell model,[23-25] were proposed for the macroscopic structure of ionic clusters to explain the SAXS results. The discrepancy in the two models comes from the structure of surroundings around the ionic core; in the two-phase model, the ionic cores exist in a liquidlike polymer matrix, but in the core–shell model they are surrounded by some ordered polymer region near the in surfaces. The present two-relaxation model for the destruction of order in the ionic clusters seems to support preferentially the core–shell model but may not necessarily contradict the two-phase model, since the ionic groups are of course bonded to the polyethylene chains in the polymer matrix.

The present model seems to explain various physical properties of ionomers well. Our dielectric results[12,13] reveal that the dielectric relaxations are closely connected with the formation of ionic clusters. In EMAA and EMAA–Zn, systems where ionic clusters are formed only to a small degree, β' and γ relaxations are observed which are ascribed to a micro-Brownian molecular motion of long

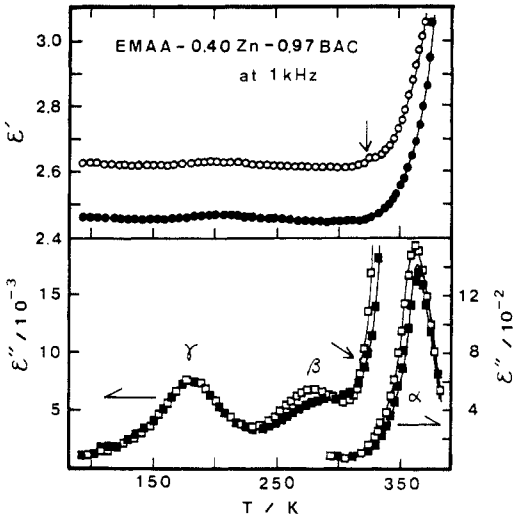

Figure 13. Temperature dependence of dielectric constant, ϵ', and the loss, ϵ'', at 1 kHz: (→) the change corresponding to the transition of ionic clusters; (○, □) unannealed sample; (●, ■) annealed sample.

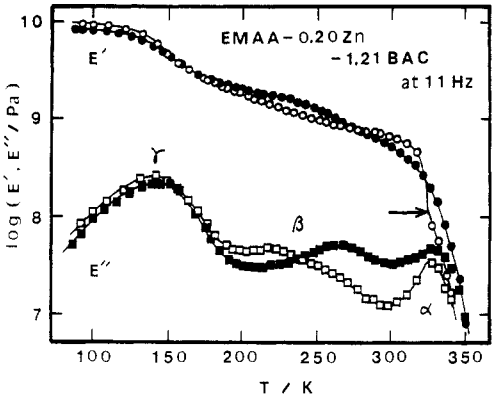

Figure 14. Temperature dependence of the dynamic, E', and the loss modulus, E'', at 11 Hz: (→) the change corresponding to the transition of ionic clusters; (○, □) unannealed sample; (●, ■) annealed sample (this sample was prepared by cooling to room temperature at the cooling rate of about 10 K/h after the annealing for 12 h at 353 K).

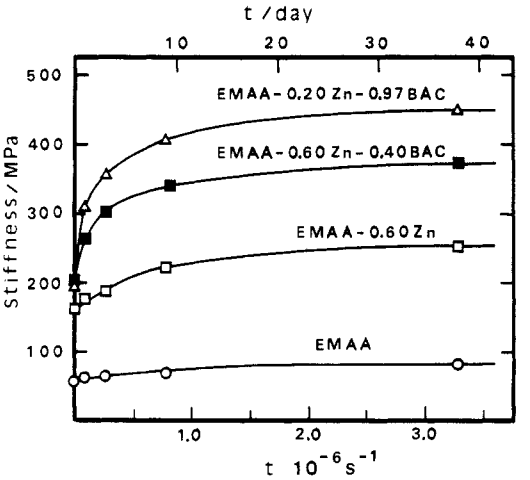

Figure 15. Change of stiffness by the storage duration, t, at 298 K for several samples quenched at a cooling rate of about 30 K/min from the molten state.

segments above T_g and a local molecular motion of short segments below T_g, respectively. In EMAA–Zn–BAC systems, the ionic clusters are formed due to the more ionized nature of $Zn(BAC)_{1-4}$–$(COO)_2$ bond. The formation of ionic clusters drastically changes the dielectric relaxations: The β' relaxation was replaced by two relaxations, α and β. The α relaxation was attributed to a micro-Brownian molecular motion of long segments containing the ionic groups of ionic clusters, because the α relaxation existed above T_i, and its magnitude was too big to be explained by the small amount of polar ionic groups not incorporated into the ionic clusters. The β relaxations was assigned to a local molecular motion of pendant carboxylic acid and zinc carboxylate groups not incorporated into the ionic clusters. Below T_i, the ordered ionic clusters prevent the micro-Brownian molecular motion of long segments by the rigid cross-linking effect, which causes the appearance of the β relaxation. Above T_i, the α relaxation takes place, since the flexible ionic groups inside of the disordered ionic clusters cooperate with the micro-Brownian molecular motion of long segments in the polymer matrix. Figure 13 shows the change of dielectric properties by annealing for EMAA–0.60Zn–0.97BAC. In the unannealed sample, the α and β relaxations are observed in the higher temperature range, which indicates the formation of ionic clusters. In the annealed sample, the β relaxation shifts to higher temperatures, compared with that in the unannealed sample, and tends to coalesce into the α relaxation. In the annealed sample, the ordered ionic clusters have not been completely formed yet, because of the long relaxation time from the disordered state to the ordered state. Therefore, the ionic clusters are considered to be so softened that the β relaxation shifts to higher temperatures. In Figure 13, a discontinuous change of ϵ' and ϵ'' is clearly seen near 325 K in the unannealed sample, although the change is very small. This change may be caused by the order–disorder transition. In the annealed sample, no discontinuous change is observed, which indicates that ordered ionic clusters are not formed. Consequently, the drastic change of the dielectric relaxation caused by the state of the ionic clusters is well explained by our model of the order–disorder transition in the ionic clusters. Mechanical studies are in progress on the present systems in our laboratory.[26] Dependence of the dynamic mechanical modulus, E' and the loss modulus, E'', against temperature at 11 Hz are shown for EMAA–0.60Zn–1.21BCA in Figure 14. In the unannealed sample, the α and β relaxations are clearly observed; this is explained by the formation of ionic clusters. On the other hand, the β relaxation shifts to higher temperatures in the annealed sample, and this can be explained by the interpretation that the ionic clusters in the annealed sample are mostly in the disordered state. The abrupt decrease of E' near 325 K for the unannealed sample corresponds to the order–disorder transition but is not observed for the annealed sample. The above results indicate that the mechanical relaxations as well as the dielectric relaxations faithfully reflect the state of the ionic clusters. Figure 15 shows plots of stiffness (modulus) against length of storage at room temperature for several samples quenched from the molten state at a rate of about 30 K/min. The formation of order in ionic clusters results in an increase of stiffness on storage. The increase is small for EMAA and for Zn(II) salts which have little tendency to form ionic clusters but is enhanced for the EMAA–xZn–yBAC systems by the formation of order in ionic clusters at room temperature. Furthermore, the value of stiffness increases with increasing content of BAC. These results also support our previous conclusion[12,13] that BAC promotes the formation of ionic clusters.

The development of ionomers containing complex Zn(II) salts with BAC allowed us to clarify the formation of ionic clusters and the presence of the order–disorder transition inside of the ionic clusters. Development and the physical

studies of ionomers functionalized by various complex metal salts with organic amine should serve to give us new information on the structure and properties of ionic clusters and are in progress in our laboratory.

Registry No. (EMAA·Zn)·BAC, 108644-30-0.

References and Notes

(1) Holiday, L. *Ionic Polymers*; Applied Science: London, 1975.
(2) Eisenberg, A.; King, M. *Ion-Containing Polymers: Polymer Physics*; Academic: New York, 1977; Vol. 2.
(3) Longworth, R. In *Developments in Ionic Polymers-1*; Wilson, D., Prosser, H. J., Eds.; Applied Science: London, 1983; Chapter 3.
(4) Pineri, M.; Eisenberg, A. *Structure and Properties of Ionomers*; NATO ASI Series; D. Reidel: Dordrecht, 1987.
(5) Ding, Y. S.; Cooper, S. L., ref 4, p 73.
(6) Ding, Y. S.; Yassuo, D. J.; Pan, H. K. D.; Cooper, S. L. *J. Appl. Phys.* **1984**, *56*, 2396.
(7) Yamauchi, J.; Yano, S. *Macromolecules* **1982**, *15*, 210.
(8) Yano, S.; Yamashita, H.; Matsushita, M.; Aoki, K.; Yamauchi, J. *Colloid Polym. Sci.* **1981**, *259*, 514.
(9) Brown, H.; Gibbs, C. F. *Ind. Eng. Chem.* **1955**, *47*, 1006.
(10) Rees, R. W. *Polym. Prepr. (Am. Chem. Soc., Div. Polym. Chem.)* **1973**, *14*, 796.
(11) Weiss, R. A.; Agawarl, P. K.; Lundberg, R. D. *J. Appl. Polym. Sci.* **1984**, *29*, 2719.
(12) Yano, S.; Tadano, K.; Sugiura, T.; Hirasawa, E., ref 4, p 481.
(13) Yano, S.; Yamamoto, H.; Tadano, K.; Yamamoto, Y.; Hirasawa, E. *Polymer* **1987**, *28*, 1965.
(14) Tadano, K.; Hirasawa, E.; Yamamoto, Y.; Yamamoto, H.; Yano, S. *Jpn. J. Appl. Phys.* **1987**, *L-24*, L1440-L1442.
(15) Edward, D.; Hayward, R. N. *Can. J. Chem.* **1968**, *46*, 3433.
(16) Bunn, C. W. *Trans. Faraday Soc.* **1939**, *35*, 482.
(17) Tsunashima, K.; Yano, S., unpublished results.
(18) Weiss, R. A. *J. Polym. Sci., Polym. Phys. Ed.* **1982**, *20*, 65.
(19) Eisenberg, A.; Trepman, E. *J. Polym. Sci., Polym. Phys. Ed.* **1978**, *16*, 1381.
(20) Kohzaki, M.; Tsujita, Y.; Takizawa, A.; Kinoshita, T. *J. Appl. Polym. Sci.* **1987**, *33*, 2393.
(21) Tsujita, Y.; Shibayama, K.; Takizawa, A.; Kinoshita, K.; Uematsu, I. *J. Appl. Polym. Sci.* **1987**, *33*, 1307.
(22) Yassuo, D. J.; Cooper, S. L. *Macromolecules* **1983**, *16*, 1871.
(23) MacKnight, W. J.; Taggart, W. P.; Stein, R. S. *J. Polym. Sci., Polym. Symp.* **1974**, *No. 45*, 113.
(24) Fujimura, M.; Hashimoto, T.; Kawai, H. *Macromolecules* **1981**, *14*, 1309.
(25) Fujimura, M.; Hashimoto, T.; Kawai, H. *Macromolecules* **1982**, *15*, 136.
(26) Hirdsawa, E.; Yamamoto, Y.; Tadano, K.; Yano, S., unpublished results.

Conformational and Packing Energy Calculations on Crystalline Isotactic 1,4-*trans*-Poly(2-methylpentadiene)

Roberto Napolitano

Dipartimento di Chimica, Università di Napoli, via Mezzocannone, 4, 80134 Napoli, Italy.

Received December 4, 1987; Revised Manuscript Received May 24, 1988

ABSTRACT: Conformational and packing energy calculations have been performed on isotactic 1,4-*trans*-poly(2-methylpentadiene) in the crystalline field. The results have been compared with experimental structure by powder X-ray diffraction. Conformational energy calculations show that only one conformation is compatible with the experimental chain axis repeat. Packing energy calculations show that the best space group is $P2_1/a$, in agreement with experimental crystal structure. The results indicate that conformational polymorphism should not be observed for the studied polymer.

Introduction

The crystal structure of isotactic 1,4-*trans*-poly(2-methylpentadiene) (PMPD) has been recently determined through best fitting of the X-ray diffraction powder profile by Brückner et al.[1] The proposed unit cell is monoclinic, space group $P2_1/c$, with $a = 4.819$ Å (chain axis), $b = 9.186$ Å, $c = 12.891$ Å, $\beta = 93.5°$, and $d_{RX} = 0.96$ g·cm^{-3} ($Z = 4$). The authors have also outlined the convenience of the analysis of X-ray diffraction data from polymer powders when obtaining oriented fibers is problematic. On the other hand, in the case of isotactic 1,4-*trans*-poly(1,3-pentadiene) (ITPP), a polymer having the same configuration and a constitution like that of PMPD, two different conformations of the polymer chain have been proposed in the crystal structures determined by X-ray analysis of oriented and unoriented samples.[2,3]

An effective approach to the determination of the structure of polymers is provided by conformational and packing energy calculations. Predictions of the conformation and of the packing stability of the chains have been performed by energy calculations for various crystalline polymers.[4-9] Also predictions of the conformation and of the crystal structure of polymers having double bonds in the main chain have been reported.[10-16] Recently conformational and packing energy calculations have been performed on ITPP[17] with the aim of elucidating the above-mentioned disagreement between the proposed X-ray structures.

The purpose of this paper is to find the most stable crystal structure of PMPD by energy calculations starting from the experimental values of the axes of the unit cell[1] and to compare the results with those obtained by X-ray analysis. The theoretical approach seems to be particularly interesting in the case of PMPD for which, at variance with ITPP, results of X-ray study on oriented fibers have not been reported nor has conformational polymorphism been found.

Conformational Energy Calculations

The conformational energy calculations have been performed on the portion of polymer chain reported in Figure 1, applying the equivalence postulate[18] along successive constitutional repeating units (CRUs) with the aim of obtaining results representative of the polymer chain in the crystalline field. The parameters for the calculations of the bending energies, torsional energies, and nonbonded interactions are those of Flory et al.,[19-21] with the exception of the force constants for the bending at the C_{sp^2} carbon atoms which have been taken from Zerbi and Gussoni.[22] As far as the nonbonded interactions are concerned, each methyl group has been considered as a single interacting atom. The intrinsic torsional potential has been taken into

0024-9297/89/2222-0233$01.50/0